*Progress In Electromagnetics Research, Vol. 138, 1–19, 2013*

# MAGNETIC FIELD SHIELDING OF UNDERGROUND CABLE DUCT BANKS

**Juan C. del Pino-López*** **and Pedro Cruz-Romero**

Department of Electrical Engineering, University of Seville, Camino de los Descubrimientos s/n, Seville 41092, Spain

**Abstract**—In this paper an in-depth parametric analysis of shielding effectiveness obtained when using ferromagnetic or conductive screens to mitigate the field generated by duct banks is presented. Due to the need of a case-by-case approach, all the simulations, performed by a finite element software (GetDp), are applied to a case study composed by 9 ($3 \times 3$) ducts, with six of them including high voltage single-core cables and the three left empty for eventual future expansion. Two shielding geometries are tested: horizontal and U-reverse, changing in each one the main parameters: width, thickness, clearance to conductors, etc. Moreover, the conductors are grouped in two balanced in-phase three-phase circuits arranged in three configurations: vertical, horizontal and triangular. The mutual phase ordering of both circuits is the one that minimizes the field, so no further field reduction can be obtained by simple methods. The power losses and cost of different shielding solutions are also presented, including the effect of adding a third circuit if required.

## 1. INTRODUCTION

During the last decades several studies have been published regarding the mitigation of magnetic field (MF) generated by underground cables, undesirable in certain circumstances (proximity of dwellings, disruptive effects in sensitive equipment, etc.) [1, 2]. In particular, an arrangement quite frequently used at low and high voltage levels is the duct bank composed by several circuits.

The simplest and cost-effective way to reduce the MF generated by cable systems is the geometric arrangement and the phase ordering. In [3] three geometric configurations are considered (stack, horizontal

*Received 17 January 2013, Accepted 8 March 2013, Scheduled 12 March 2013*

* Corresponding author: Juan Carlos del Pino-Lopez (vaisat@us.es).

and triangular), obtaining a highest MF ratio of 32.6 between the worst and better configurations. In [4] other conductor arrangements are considered, obtaining a highest MF ratio of 29.3. It is clear that this method is highly effective and that should be the first one to be applied. However, if higher reduction is required, one should turn to additional procedures, like the use of shielding [5–8].

Regarding the use of magnetic shields to reduce the MF of duct banks, there is little research so far. In fact we have found just the paper [9] that deals with this topic, where the horizontal and U-reverse magnetic shields are analysed for the case of a $3 \times 3$ duct bank with two triangular balanced three-phase circuits.

This paper goes one step further because not only the ferromagnetic but also the conductive (aluminium) shield is analysed, delving deeper in the parametric analysis (width, thickness, clearance to conductors, etc.) of the shield, the losses and the global cost of each solution. The analysis is not restricted to triangular configuration, but also to vertical and horizontal. Moreover, the effect on the MF due to a further addition of a third circuit is analysed in depth, comparing all the possible configurations that result, selecting those conductors configurations that are the optimum with regard to MF generation.

## 2. ELECTROMAGNETIC FIELD EQUATIONS

The MF obtained when shielding a group of power cables must be computed by solving Maxwell's equations. Due to their geometrical shape and material properties, this requires numerical techniques, such as the finite element method (FEM) [10–13], which is applied in this work by using a free commercial FEM software called GetDp [14].

The mathematical model to be solved is based on the following assumptions:

1) The cables are straight and infinitely long, thereby rendering the problem 2-D.
2) The electrical conductivity of mother soil is ignored.
3) The phase currents are sinusoidal and balanced.
4) The sheath current is neglected (single point grounded system).

In this situation, the equation to be solved can be described as

$$\nabla \times \left( \frac{1}{\mu} \nabla \times \vec{A} \right) + j\omega\sigma\vec{A} = \vec{J}_e \tag{1}$$

where $\vec{A}$ is the magnetic vector potential, $\omega$ is the angular frequency, $\sigma$ is the conductivity, $\mu$ is the permeability and $\vec{J}_e$ is the external current density.

The degree of mitigation achieved by various shielding schemes is evaluated by the term shielding effectiveness (SE), which is defined as the ratio between the resulting (root sum square) nonmitigated and mitigated MFs in dB:

$$\mathrm{SE}(x,y) = 20 \cdot \log\left(\frac{\left|\vec{B}_p(x,y)\right|}{\left|\vec{B}_s(x,y)\right|}\right) \tag{2}$$

where $\vec{B}_p$ is the MF generated by the power cables, and $\vec{B}_s$ is the mitigated field.

The power losses generated in the shield will be also computed. In particular, for conductive shields, eddy current losses ($P_e$) can be calculated from the total current density $\vec{J}$ as follows:

$$P_e = \int \frac{\vec{J} \cdot \vec{J}^*}{\sigma} dS \tag{3}$$

On the other hand, the total losses ($P_{loss}$) generated in nonlinear ferromagnetic materials are separated into three loss components, known as the hysteresis $P_h$, classical eddy current $P_e$, and additional losses $P_a$ [15–17], being

$$P_{loss} = P_h + P_e + P_a = K_h f^a B_m^b + P_e + K_a f^{1.5} B_m^{1.5} \tag{4}$$

where $P_e$ can be computed by (3), $B_m$ is the maximum flux density, $K_h$ is the hysteresis loss coefficient, $K_a$ is the additional loss coefficient, and $a$ and $b$ are constants.

## 3. CASE STUDY

To show the complex casuistry that occurs when shielding a duct bank with multiple circuits, the case of a typical $3 \times 3$ buried duct bank is analysed. The main geometrical magnitudes of the system are represented in Fig. 1. A 132 kV double circuit line is considered to be installed in the duct bank, with phase conductors having a cross-section of 630 $\mathrm{mm}^2$ and a current of 750 A (the three-phase currents in both circuits are in phase). Phase conductors can be placed following well known MF management techniques to reduce the MF in the area above the ground surface [3]. Bearing this in mind, three representative configurations have been selected for this study: vertical, horizontal and triangular formations (Fig. 2). The MF values obtained in these situations, at a point situated at 1 m above ground surface, are presented in Table 1. We will assume that three ducts are left empty for future expansions, to place communication lines, etc.

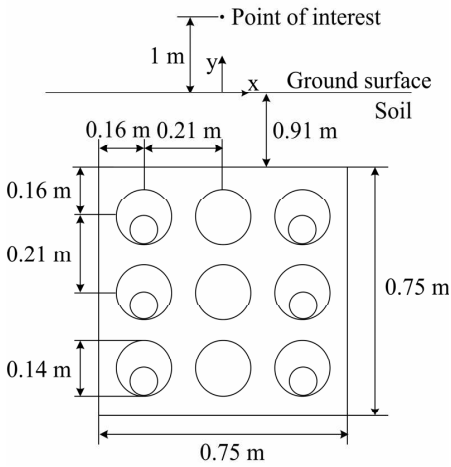


**Figure 1.** Geometrical configuration of the duct bank.

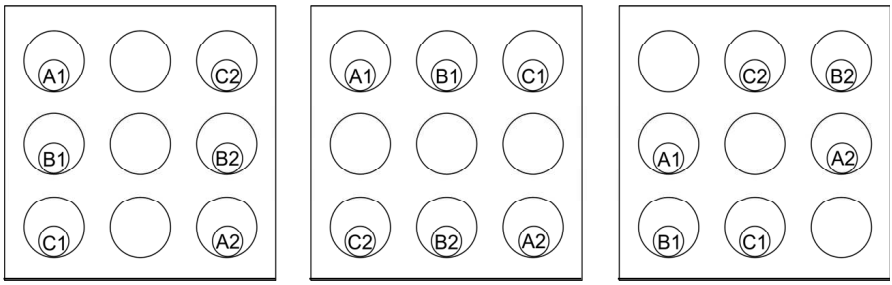


**Figure 2.** (a) Vertical, (b) horizontal and (c) triangular arrangements.

**Table 1.** Magnetic field at the point of interest (1 m above ground surface) in the three arrangements considered.

| Arrangement | $B$ (μT) |
|---|---|
| Vertical | 5.42 |
| Horizontal | 5.45 |
| Triangular | 3.98 |

Other configurations may provide lower MF values, but having the power cables closer, which leads to an important current carrying capacity reduction of the line. Thus, they are not considered in this work.

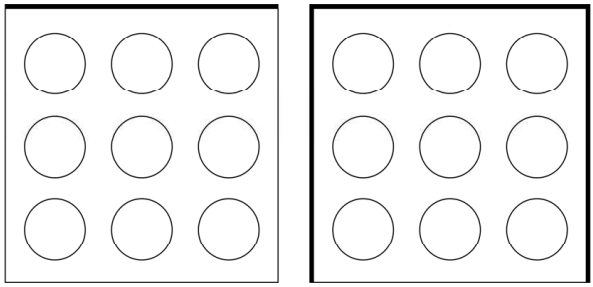


**Figure 3.** (a) Horizontal plate and (b) reverse-U in the duct bank.

**Table 2.** Parameters for the various materials used in the shield.

| Material | Density (kg/m$^3$) | $\sigma$ (S/m) | $\mu_r$ | $K_h$ | $a$ | $b$ | $K_a$ |
|---|---|---|---|---|---|---|---|
| Al | 2700 | $38 \cdot 10^6$ | 1 | – | – | – | – |
| LCS | 7580 | $6.5 \cdot 10^6$ | $\mu_r\ (B)$ | 0.045 | 1.15 | 1.35 | 0.0045 |

If lower MF levels are required, metallic shields can be installed next to the duct bank. The most usual ones are the horizontal plate and the reverse-U [2]. Both types of shield provide good MF levels when shielding power cables installed in flat configuration with conductive materials (e.g., aluminium) [5], but it is not clear how do they work when shielding a duct bank (Fig. 3), and which is the best material to be employed (conductive or ferromagnetic) depending on the phase arrangement used in the circuits.

To clarify this, both shield shapes are studied next when installed in the $3 \times 3$ duct bank employing two materials: aluminium (Al) and a low carbon steel (LCS). Their main parameters are shown in Table 2, which includes the coefficients needed to compute the hysteresis and additional losses by Equation (4) (provided by the manufacturer). Since LCS is a nonlinear ferromagnetic material, its relative permeability is considered as a function of the flux density $\mu_r(B)$, as shown in Fig. 4.

The size and position of both shield shapes are initially considered to be the following: a horizontal plate located at the top surface of the duct bank with the same width (75 cm) and a thickness of 3 mm (Fig. 3(a)); a reverse-U shield covering the duct bank with the same width and height (75 cm) and 3 mm thick (Fig. 3(b)). Both shield configurations are taken as the reference settings to be used in the parametric analysis developed next.

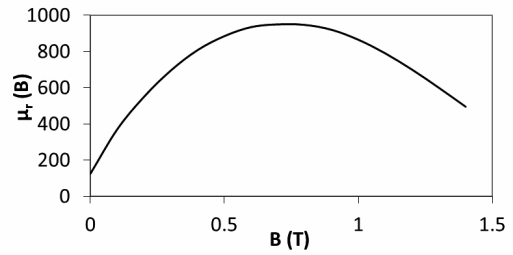


**Figure 4.** Relative permeability of the low carbon steel.

## 4. PARAMETRIC ANALYSIS

An in-depth parametric analysis is developed in order to show the influence of the geometrical parameters of the selected shields not only on the mitigation achieved at the point of interest, situated at 1 m above ground surface (Fig. 1), but also on the power losses induced in the shields. Only one dimension is revised at the time, leaving the other dimensions at the reference values defined previously, and considering the vertical (V), horizontal (H) and triangular (T) arrangements selected earlier (Fig. 2).

### 4.1. Horizontal Plate

*4.1.1. Influence of Shield Thickness*

The influence of the shield thickness on the SE is shown in Fig. 5(a), where V-LCS designates a LCS shield placed in a duct bank where phases are installed in a vertical arrangement (Fig. 2(a)). As can be seen, the SE improves with the thickness in all the materials and situations analysed (Fig. 5(a)), but it remains almost constant from a certain value. Another aspect to be remarked is that the SE obtained by each material in the vertical and horizontal arrangements are quite similar, although the best mitigation results are obtained when aluminium is used, being the steel shield more interesting when the phases are in triangular configuration. However, these conclusions may change when the other dimensions are modified, as it is shown in further sections.

Regarding the power losses (Fig. 5(b)), it is easily observed that they are nearly constant in the LCS, while they strongly decreases in the aluminium shields. Furthermore, power losses are usually higher in the ferromagnetic shields. In any case, it should be noticed that, for each material, the lowest power losses are induced if the phase

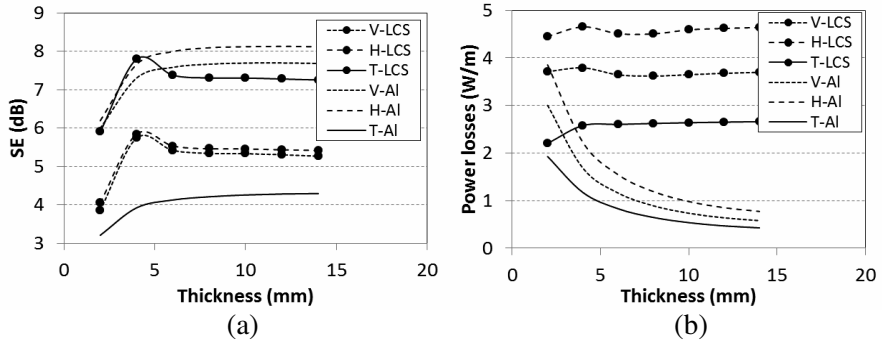


**Figure 5.** Influence of the shield thickness on (a) the SE and (b) the power losses induced on a horizontal plate.

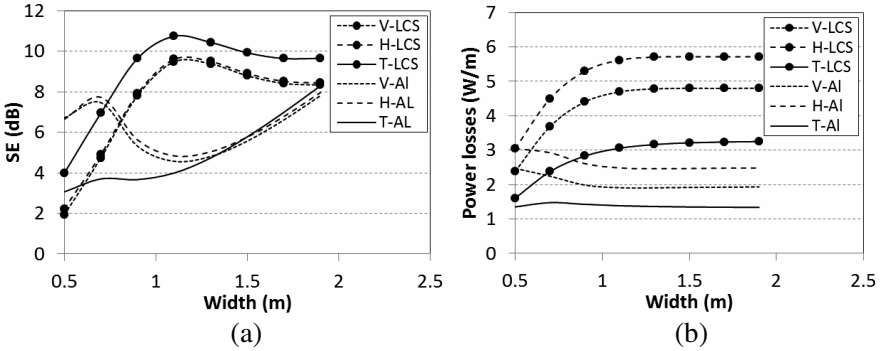


**Figure 6.** Evolution of (a) SE and (b) power losses with the shield width (horizontal plate).

conductors are laid in a triangular arrangement, and the highest when they are configured in a vertical one.

### *4.1.2. Influence of Shield Width*

For a 3 mm thick shield situated at the top surface of the duct bank, the SE provided by aluminium and LCS shields evolve in quite different ways when its width is increased, as can be observed in Fig. 6(a).

In particular, the SE of the LCS shield improves with the width, achieving a maximun at 1.1 m, while it even worsens in the case of aluminium shields, which get better SE values when using shorter or longer widths, but always achieving lower mitigation levels than those of the LCS shields. So, contrary to what was suggested in the previous

section, the LCS shield seems to be the best choice for all the phase arrangements considered if the appropriate width is selected. Also, this behavior is extremely related to other parameters, such as the distance between the plate and the top surface of the duct bank, leading to new conclusions as it is explained in the next section.

In any case, the influence of the shield width on the power losses induced in the shield is as shown in Fig. 6(b), where it can be observed how they increase until a certain value in the LCS shields, while these losses are getting lower in the aluminium shields. Again, lower losses are induced in the conductive material when increasing the shield size. Also, as observed in the previous section, lower losses are induced in both shield materials when phases are placed in a triangular formation, whereas they are more important when phases are placed in a vertical configuration.

### *4.1.3. Influence of the Duct Bank-shield Separation*

The results obtained in the previous section are derived from a situation in which the shield is resting on the top surface of the duct bank. But if the shield is moved up a certain distance, different conclusions are obtained. In this sense, Figs. 7(a) and 7(b) show the influence of the duct bank-shield distance on the SE achieved for two values of the shield width: 0.75 m and 1.5 m.

It is easily observed that both figures show quite different behaviors of the SE. For example, in the shortest shield (Fig. 7(a)), the SE gets worsen in all the arrangements analysed when LCS shields are getting farther from the duct bank, but aluminium shields improve its efficiency, having a maximum at about 0.1 m of separation. The

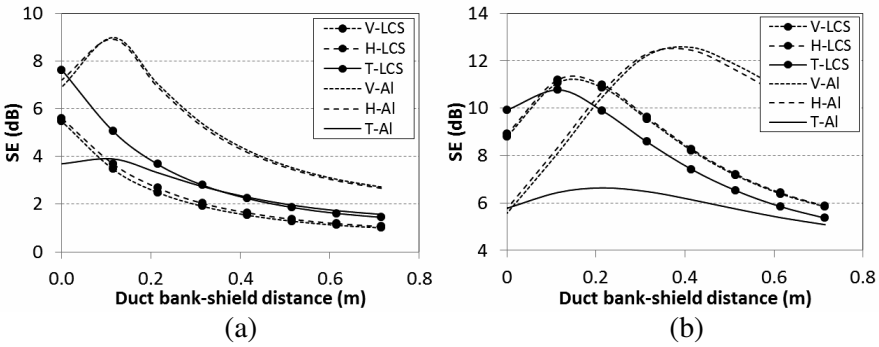


**Figure 7.** Evolution of SE with the duct bank-shield distance for a shield width of (a) 0.75 m and (b) 1.5 m (horizontal plate).

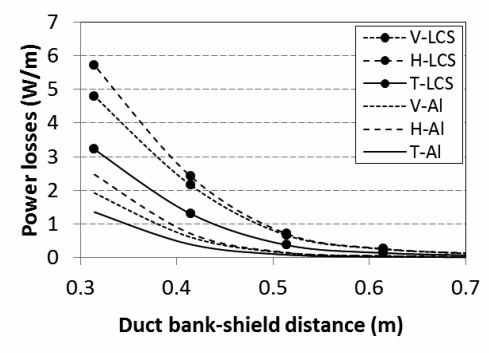


**Figure 8.** Evolution of the shield losses with the duct bank-shield distance for a shield width 1.5 m (horizontal plate).

latter is also observed in larger shields (Fig. 7(b)), since both materials provide better mitigation results when the shield is separated to a certain distance from the duct bank.

Consequently, for each situation (phase arrangement and shield material) there is an ideal combination of values for the shield width and its separation from the duct bank that maximizes the SE. However, for obtaining these values, the geometrical and technical constraints associated to the final location must be also considered.

One aspect that can help to take decisions in this matter are the power losses induced in the shield. For example, Fig. 8 shows the evolution of these losses with the duct bank-shield distance for a shield width of 1.5 m. As can be observed, power losses decrease with this parameter in all the cases, and lower values are induced again in both materials when the circuits are placed in triangular formation. Thus, it is of interest to place the shield at a certain distance from the duct bank not only to achieve better MF values, but also to reduce the induced losses.

## 4.2. Reverse-U

In this case, there are more geometrical parameters involved, difficulting the analysis of the results to obtain simple conclusions.

### *4.2.1. Influence of Shield Thickness and Width*

As observed in the horizontal plate, increasing the thickness leads to better mitigation results in all the phase arrangements considered, as

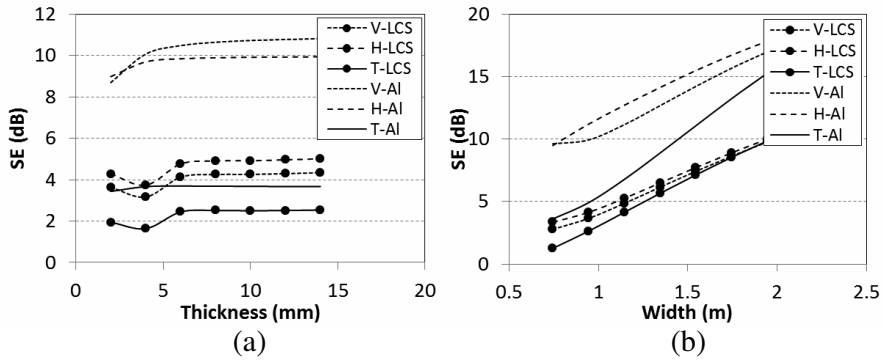


**Figure 9.** Influence of (a) the shield thickness and (b) the shield width on the SE (reverse-U).

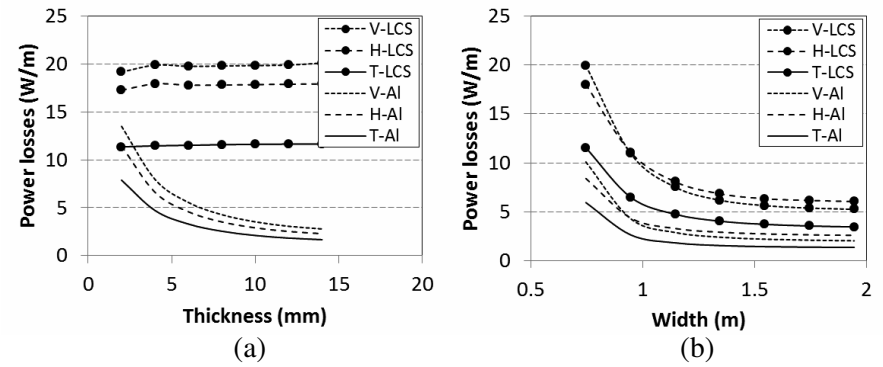


**Figure 10.** Influence of (a) the shield thickness and (b) the shield width on the power losses induced in the shield (reverse-U).

shown in Fig. 9(a), although the SE remains almost constant for values higher than 7 mm in all the cases.

In addition, Fig. 9(b) shows that better mitigation levels are achieved in all the situations if wider shields are used. Furthermore, from both figures it can be concluded that an aluminium shield would be the best choice to be installed in the duct bank, independently of the phase arrangement employed. Nonetheless, as observed in the case of the horizontal plate, this conclusion may change when the rest of the geometrical parameters are taken into account.

About the shield losses, Figs. 10(a) and 10(b) show its evolution with both parameters. The influence of the shield thickness is very similar to that observed in the case of the horizontal plate, but the

influence of the shield width is rather different to that case, since now power losses decrease strongly with this parameter in all the situations. Besides, it is again observed that lower losses are induced in the shield (either of aluminium or LCS) when the phases are arranged in a triangular formation.

### *4.2.2. Influence of Shield Height*

In the reverse-U shield there is a new parameter to be considered: the height of the vertical sections of the shield. Its influence on the SE achieved at the point of interest is shown in Fig. 11(a).

As can be seen, when the shield is resting on the top surface of the duct bank (as it is the case) the SE decreases with this parameter, achieving a minimum from which SE increases again. This is observed in all the situations, concluding that, for this particular position of the shield, LCS shields provide better results when the shield height is lower than 0.3 m, and aluminium shields are the best choice when using a higher height. However, this conclusion may be influenced by other parameters. In any case, it must be remarked that selecting the wrong settings may lead to negative SE values as those observed in Fig. 11(a), which means that the MF in the interest point has increased over the MF previous to the shielding.

On the other side, the shield losses increase with this parameter, as shown in Fig. 11(b), where lower values are obtained again when phases are placed in triangular formation.

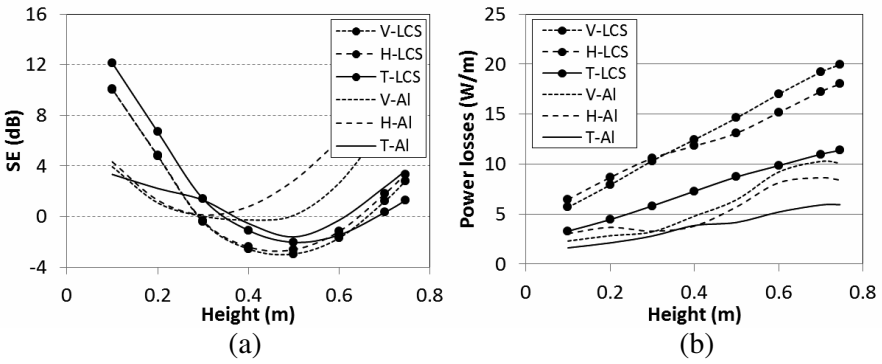


**Figure 11.** Evolution of (a) the SE and (b) the power losses with the shield height (reverse-U).

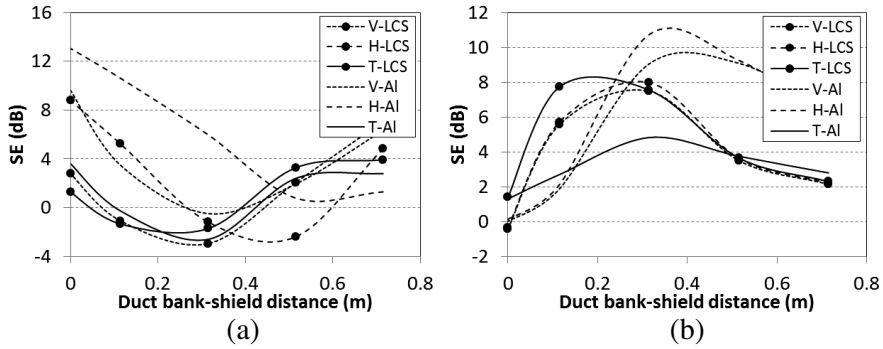


**Figure 12.** Evolution of SE with the duct bank-shield distance for a shield height of (a) 0.75 m and (b) 0.3 m (reverse-U).

*4.2.3. Influence of the Duct Bank-shield Separation*

As observed in the horizontal plate, the distance between the top surface of the duct bank and the horizontal section of the shield is strongly related to the rest of the parameters. This is observed again for the reverse-U shield, as shown in Figs. 12(a) and 12(b), where the evolution of the SE for two values of the shield height (0.75 m and 0.3 m) are represented.

As can be seen, the SE evolves in a very different way on both situations. In particular, Fig. 12(a) shows how the SE worsens when the duct bank-shield distance is increased, having a negative minimum from which the SE improves again. However, if the shield has a shorter height (Fig. 12(b)), the SE achieves a maximum when the shield is farther from the duct bank. So, again, the suitable position and size for the shield that maximizes the SE on each material and phase configuration must be found.

On the other side, the influence of the duct bank-shield distance on the power losses induced in the shields is very similar to that observed in the case of the horizontal plate (Fig. 8), where they decrease strongly with this parameter, being less important in the situation in which phases are in a triangular arrangement.

### 4.3. MF at the Edges of the Right-of-way

Previous analyses are focused on minimizing the MF in the area directly above the cables. But one unexpected issue observed in [9] arises also in this work, as shown in Fig. 13, where it is represented the SE profile provided by the horizontal plate and the reverse-U (made

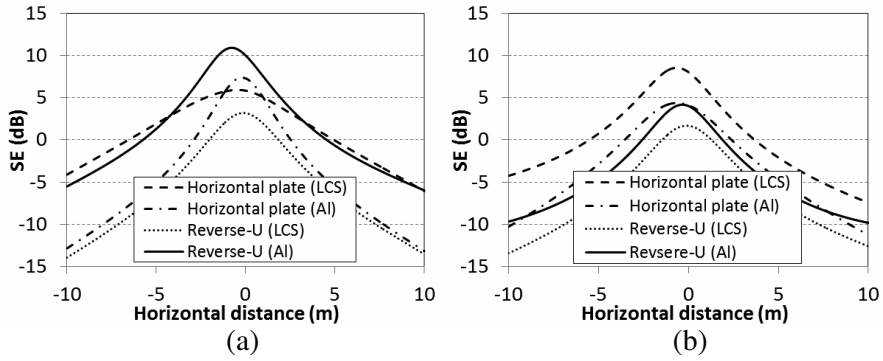


**Figure 13.** SE profile provided by different shields at 1 m above ground surface for the (a) vertical and (b) triangular arrangement.

of aluminium and LCS with the reference dimensions) at 1 m above ground surface when phases are arranged in vertical and triangular formation (results of the horizontal case are similar to the vertical configuration). As can be seen, the SE decreases with distance, achieving negative values at a certain distance. This means that the presence of the shield increases the MF in the edges of the right-of-way. This effect is less important in those configurations which provide higher SE values (e.g., the aluminium reverse-U in the vertical case and the LCS horizontal plate in the triangular case), with about $-5$ dB at 10 m from the trench axis. But the less effective shield configurations provide SE values close to $-15$ dB, which means a MF about 6% higher than the initial situation without shield. Nevertheless, at far distances the MF is already low, so this increase may not exceed the mitigation requirements. Hence, it is clear that the design process should be carefully developed in order to guarantee the MF requirements in the whole region to be protected.

## 5. INSTALLATION OF A NEW LINE IN THE DUCT BANK

Once a shield is installed in a duct bank, where the phase conductors are placed in a particular arrangement, more circuits could be placed in the empty ducts with the increase of electricity consumption. This circumstance may lead to an inefficient performance of the installed shield, so it is of interest to study this new situation previously in the design process of the shield, analysing how the new circuits should be placed in the duct bank in order to preserve the mitigation

requirements. This is studied next for the case study presented in Section 3 (Fig. 2). The current flowing through this new circuit is considered to be the same as that flowing through the existing circuits (750 A).

### 5.1. Horizontal Plate

A 6 mm thick horizontal plate located at the top surface of the duct bank, having a width of 75 cm (Fig. 3(a)), is considered in this analysis. The phases of the new circuit can be placed into the empty ducts in different configurations, depending on how the existing phases are already installed. This leads to six different combinations on each arrangement, which are shown in Table 3 (the new circuit is typed in bold). For every phase arrangement and shield material, Table 3 also shows the MF values obtained in the point of interest, where those arrangements that lead to the lowest MF values for each material are

**Table 3.** MF (in μT) at the point of interest for each shield material and phase arrangement.

| Vertical | | | Horizontal | | | Triangular | | |
|---|---|---|---|---|---|---|---|---|
| Case | LCS | Al | Case | LCS | Al | Case | LCS | Al |
| A **A** C | | | A B C | | | **A** C B | | |
| B **B** B | 11.13 | 13.57 | **A B C** | 14.49 | 7.81 | A **B** A | 15.72 | 13.37* |
| C **C** A | | | C B A | | | B C **C** | | |
| A **C** C | | | A B C | | | **C** C B | | |
| B **A** B | 11.31 | 14.59 | **C A B** | 11.55 | 10.61 | A **A** A | 17.28 | 16.19 |
| C **B** A | | | C B A | | | B C **B** | | |
| A **B** C | | | A B C | | | **B** C B | | |
| B **C** B | 10.41 | 12.35* | **B C A** | 10.04 | 9.16 | A **C** A | 14.96 | 17.04 |
| C **A** A | | | C B A | | | B C **A** | | |
| A **C** C | | | A B C | | | **C** C B | | |
| B **B** B | 10.45 | 13.68 | **C B A** | 9.31* | 10.67 | A **B** A | 16.96 | 17.92 |
| C **A** A | | | C B A | | | B C **A** | | |
| A **A** C | | | A B C | | | **A** C B | | |
| B **C** B | 11.14 | 14.64 | **A C B** | 13.98 | 9.28 | A **C** A | 17.23 | 14.37 |
| C **B** A | | | C B A | | | B C **B** | | |
| A **B** C | | | A B C | | | **B** C B | | |
| B **A** B | 10.25* | 12.39 | **B A C** | 12.74 | 7.59* | A **A** A | 14.91* | 15.32 |
| C **C** A | | | C B A | | | B C **C** | | |

*Best configuration

**Table 4.** MF and SE at the point of interest, shield losses ($P_{loss}$) and the total cost of a horizontal plate (100 m length) for every material and phase arrangement when there are two circuits (2C) or three circuits (3C).

| Material | | Vertical | | Horizontal | | Triangular | |
|---|---|---|---|---|---|---|---|
| | | 2C | 3C | 2C | 3C | 2C | 3C |
| LCS | SE (dB) | 5.42 | 2.93 | 5.53 | −0.21 | 3.38 | 1.45 |
| | MF (μT) | 2.68 | 10.25 | 2.78 | 9.31 | 1.63 | 14.91 |
| | $P_{loss}$ (W/m) | 3.64 | 4.95 | 4.5 | 2.6 | 2.6 | 1.32 |
| | Cost (€) | 8,207 | 10,429 | 9,666 | 6,443 | 6,443 | 4,272 |
| Al | SE (dB) | 7.58 | 1.31 | 8 | 7.14 | 4.13 | 3.07 |
| | MF (μT) | 2.17 | 12.35 | 2.09 | 7.59 | 2.37 | 13.37 |
| | $P_{loss}$ (W/m) | 1.16 | 1.58 | 1.54 | 2.7 | 0.83 | 1.91 |
| | Cost (€) | 5,105 | 5,818 | 5,750 | 7,717 | 4,545 | 6,377 |

selected. From this selection it is derived the way in which the phases of the new circuit must be placed for obtaining the lowest MF possible.

To show how the presence of the new line influences on the shield performance, Table 4 shows the values of the MF and the SE in the initial situation, with two circuits in the duct bank (2C), and in the new situation, with three circuits (3C). The 3C cases are the best configurations selected from Table 3. Table 4 also shows the total cost of the shields (material and losses) considering a line length to be shielded of 100 m, over an operation period of 30 years as stated in the IEC 60287 for the cost of power cables [18]. Reference data are: 2600 euro/t for aluminium; 600 euro/t for LCS; energy price: 0.1 euro/ton; discount rate: 5%; energy cost rate: 2%; and demand charge: 0.03 euro/W·year.

As can be seen, the MF levels increase intensively when the new circuit is installed. Also, in certain cases the SE strongly decreases compared to the initial situation (2C). This happens in the vertical arrangement for both shield materials, but particularly when using aluminium (from 7.58 dB to 1.31 dB). In any case, both materials provide similar MF levels, so the best choice for this arrangement would be the aluminium shield since it has the lowest cost.

For the horizontal arrangement, Table 4 shows that the SE of the LCS shield decreases to negative values, although the new circuit is placed to minimize the MF levels (as obtained from Table 3). So, the aluminium shield would be the best choice in this particular circumstance.

Finally, in the triangular formation, the SE of both materials also decreases, providing similar MF levels. But the lower losses of the LCS shield make this option to be the most interesting choice due to the lower cost.

### 5.2. Reverse-U

In this case, a 6 mm thick reverse-U shield located at the top surface of the duct bank is considered, having a width and height of 0.75 m (Fig. 3(b)). Again, all the possible locations to place the new phases have been analysed in a similar way to that shown in Table 3, selecting, for the sake of simplicity, those configuration that provide the lowest MF values depending on the phase arrangement and the shield material. Those selected configurations are shown in Table 5 with their resulting MF and SE values, comparing the initial (2C) and final (3C) situations. Also, the losses and the total cost associated to the shields are shown.

As can be seen, when the new circuit is placed, the selected arrangements lead to much better values of SE in all the situations analysed. Consequently, and contrary to what happens in the horizontal plate, it is possible to achieve MF values close to those obtained when there were only two circuits installed. In some cases, it is even possible to achieve lower values with both materials, as shown in Table 5 for the horizontal arrangement.

**Table 5.** MF and SE provided at the point of interest, and the power losses ($P_{loss}$) and the total cost of a reverse-U shield (100 m length) for each material and phase arrangement when there are two circuits (2C) or three circuits (3C).

| Material | | Vertical | | | Horizontal | | | Triangular | | |
|---|---|---|---|---|---|---|---|---|---|---|
| | | 2C | 3C | | 2C | 3C | | 2C | 3C | |
| LCS | SE (dB) | 4.12 | 10.76 | A**A**C<br>B**C**B<br>C**B**A | 4.76 | 17.04 | ABC<br>**BAC**<br>CBA | 2.44 | 16.5 | **C**CB<br>**AA**A<br>BC**B** |
| | MF (μT) | 3.23 | 4.84 | | 3.04 | 2.42 | | 2.87 | 3.46 | |
| | $P_{loss}$ (W/m) | 19.74 | 28.12 | | 17.77 | 31.51 | | 11.51 | 35.93 | |
| | Cost (€) | 39,624 | 53,838 | | 36,282 | 59,589 | | 25,663 | 67,086 | |
| Al | SE (dB) | 10.48 | 14.66 | A**C**C<br>B**A**B<br>C**B**A | 9.84 | 18.43 | ABC<br>**BCA**<br>CBA | 3.69 | 20.75 | |
| | MF (μT) | 1.55 | 3.08 | | 1.69 | 1.47 | | 2.49 | 2.17 | |
| | $P_{loss}$ (W/m) | 5.55 | 6.6 | | 4.58 | 6.83 | | 3.29 | 6.76 | |
| | Cost (€) | 18,891 | 20,672 | | 17,245 | 21,062 | | 15,057 | 20,943 | |

In conclusion, for the shield configuration analysed, it is clear that the reverse-U shield is capable of maintaining the MF requirements even if a future expansion is accomplished in the duct bank. However, the high losses induced in the reverse-U make this type of shield much more expensive than the horizontal plate. Furthermore, the shield losses are more important in all the situations when a new circuit is placed in the duct bank, and thus its total cost, especially in the LCS shield. Therefore, from Table 5 it can be derived that the aluminium shield is the best choice for all the phase arrangements considered, since it provides the lowest MF values at the lowest cost.

## 6. CONCLUSIONS

The shielding effectiveness of two types of open shields (a horizontal plate and a reverse-U) has been studied when installed over an underground duct bank. In particular a $3 \times 3$ duct bank has been considered, where a 132 kV double circuit is placed in three different arrangements which cause the lowest MF levels above ground surface: vertical, horizontal and triangular.

An in-depth parametric analysis has been developed on both shield shapes in order to show the influence of its geometrical parameters on the SE achieved and on the power losses induced in the shield. This helps to select the suitable material and dimensions of the shield to be placed near a particular phase arrangement. However, the results obtained from this analysis show that all parameters are strongly related to each other, making this task more difficult, being necessary to consider the geometrical and technical constraints related to the final location.

In any case, it is derived from this analysis that it may be of interest to separate the shield from the duct bank in order to maximize the SE, selecting the suitable width to achive this goal. This also leads to lower losses in the shield, something that also happens if the phases are arranged in a triangular formation, independently of the material employed in the shields.

It is also observed that the MF at the edges of the right-of-way may be negatively affected by the presence of the shields, leading to higher MF values than the initial situation without shield.

On the other hand, if a third circuit is to be placed in the duct bank, it is concluded that the SE of the horizontal plate usually gets worse, while the efficiency of the reverse-U shield strongly improves, providing MF levels close to those achieved when only two circuits are in the duct bank. However, the power losses induced in the reverse-U are quite important, and thus its cost.

## ACKNOWLEDGMENT

This work has been supported by the Spanish Ministry of Science & Innovation under grant ENE2010-18867 and by the regional Government of Andalucía under grant P09-TEP-5170.

## REFERENCES

1. Conti, R., F. Donazzi, P. Maioli, R. Rendina, and E. A. Sena, "Some Italian experiences in the utilization of HV underground cable systems to solve local problems due to magnetic field and other environmental issues," *Cigré Session*, Paper C4-303, 2006.
2. Working Group C4.02.04, *Mitigation Techniques of Power-frequency Magnetic Fields Originated from Electric Power Systems*, 373, Cigré TB, 2009.
3. Dawoud, M. M., I. O. Habiballah, A. S. Farag, and A. Fironz, "Magnetic field management techniques in transmission underground cables," *Electric Power Systems Research*, Vol. 48, 117–192, 1999.
4. Karady, G. G., C. V. Nunez, and R. Raghavan, "The feasibility of magnetic field reduction by phase relationship optimization in cable systems," *IEEE Trans. on Power Delivery*, Vol. 13, No. 2, Apr. 1998.
5. Del Pino, J.-C. and P. Cruz, "Influence of different types of magnetic shields on the thermal behaviour and ampacity of underground power cables," *IEEE Trans. on Power Delivery*, Vol. 26, No. 4, 2659–2667, 2011.
6. Boyvat, M. and C. Hafner, "Molding the flow of magnetic field with metamaterials: Magnetic field shielding," *Progress In Electromagnetics Research*, Vol. 126, 303–316, 2012.
7. Sergeant, P. and S. Koroglu, "Electromagnetic losses in magnetic shields for buried high voltage cables," *Progress In Electromagnetics Research*, Vol. 115, 441–460, 2011.
8. Del Pino, J. C., P. Cruz, and L. Serrano-Iribarnegaray, "Impact of electromagnetic losses in closed two-component magnetic shields on the ampacity of underground power cables," *Progress In Electromagnetics Research*, Vol. 135, 601–625, 2013.
9. Bascom, E.-C., W. Banker, and S. A. Boggs, "Magnetic field management considerations for underground cable duct banks," *IEEE Transmission & Distribution Conference, 2005/2006 IEEE PES*, 414–420, 2006.
10. Xu, X.-B. and G. Liu, "A two-step numerical solution of magnetic

field produced by ELF sources within a steel pipe," *Progress In Electromagnetics Research*, Vol. 28, 17–28, 2000.

11. Gómez-Revuelto, I., L. E. García-Castillo, and M. Salazar-Palma, "Goal-oriented self-adaptive HP-strategies for finite element analysis of electromagnetic scattering and radiation problems," *Progress In Electromagnetics Research*, Vol. 125, 459–482, 2012.
12. Torkaman, H. and E. Afjei, "Comparison of three novel types of two-phase switched reluctance motors using finite element method," *Progress In Electromagnetics Research*, Vol. 125, 151–164, 2012.
13. Cabanas, M. F., F. Pedrayes González, M. G. Melero, C. H. Rojas García, G. A. Orcajo, J. M. Cano Rodríguez, and J. G. Norniella, "Insulation fault diagnosis in high voltage power transformers by means of leakage flux analysis," *Progress In Electromagnetics Research*, Vol. 114, 221–234, 2011.
14. GetDp, Version 2.2.1, P. Dular and C. Geuzaine (University of Liège), http://www.geuz.org/getdp/, 2012.
15. Bertotti, G., *Hysteresis in Magnetism*, Academic Press, San Diego, 1998.
16. Öztürk, N. and E. Çelik, "Application of genetic algorithms to core loss coefficient extraction," *Progress In Electromagnetics Research M*, Vol. 19, 133–146, 2011.
17. Mahmoudi, A., N. A. Rahim, and W. P. Hew, "Axial-flux permanent-magnet motor design for electric vehicle direct drive using sizing equation and finite element analysis," *Progress In Electromagnetics Research*, Vol. 122, 467–496, 2012.
18. IEC Standard 60287, *Electric Cables — Calculation of the Current Rating — Part 3-2: Sections on Operating Conditions — Economic Optimization of Power Cable Size*, 2nd editon, 2006.